

Low-energy phonon excitations in superconducting $R\text{Ni}_2\text{B}_2\text{C}$ ($R=\text{Lu}, \text{Y}$)

M. Bullock, J. Zarestky, C. Stassis, A. Goldman, and P. Canfield

Ames Laboratory and Department of Physics and Astronomy, Iowa State University, Ames, Iowa 50011

Zentaro Honda and Gen Shirane*

The Institute of Physical and Chemical Research (RIKEN), Wako, Saitama 351-01, Japan

S. M. Shapiro

Brookhaven National Laboratory, Upton, New York 11973-5000

(Received 9 May 1997; revised manuscript received 8 September 1997)

Inelastic neutron-scattering techniques have been used to study the low-energy phonon excitations in superconducting $R\text{Ni}_2\text{B}_2\text{C}$ ($R=\text{Lu}, \text{Y}$) to further characterize the anomalous features observed by Kawano *et al.* [Phys. Rev. Lett. **77**, 4628 (1996)] for $R=\text{Y}$ and Stassis *et al.* [Phys. Rev. B **55**, R8678 (1997)] for $R=\text{Lu}$, when these systems enter the superconducting ground state. We find that above T_c the frequencies of the $\Delta_4[\xi 00]$ lowest-lying acoustic and optic phonon modes decrease with decreasing temperature, for ξ close to the nesting vector ξ_m . In addition there is a shift of intensity from the upper to the lower mode, an effect characteristic of mode coupling. The observed intensity transfer between these modes above T_c can be described satisfactorily in both compounds by a coupled-mode model. Below T_c the observed spectrum changes dramatically: it consists of a sharp peak at approximately 4 meV with a broad weak shoulder at higher energies. The experimental results unambiguously show that this dramatic change is due to the onset of superconductivity in these compounds. In this temperature region, the results are in qualitative agreement with recent theoretical calculations. [S0163-1829(98)04713-4]

I. INTRODUCTION

The physical properties of the rare-earth nickel boride carbides ($R\text{Ni}_2\text{B}_2\text{C}$, $R=\text{rare earth}$) are of considerable interest.¹⁻⁴ Their crystal structure³ is body-centered tetragonal (space group $I4/mmm$), with $a \approx 3.5 \text{ \AA}$ and $c \approx 3a$, and consists of $R\text{-C}$ layers separated by Ni_2B_2 sheets. Many of these compounds are superconductors with relatively high superconducting temperatures. Among these superconductors, the nonmagnetic Lu and Y compounds exhibit²⁻⁵ the highest superconducting temperatures, 16.5 K and 15.5 K, respectively. Of particular interest is that in several of these compounds ($R=\text{Tm}, \text{Ho}, \text{Er}, \text{and Dy}$) superconductivity coexists with magnetic order.²⁻⁷

To obtain some insight into the subtle interplay between superconductivity and magnetism, the magnetic structures of these compounds have been studied extensively by neutron and x-ray scattering techniques on both single crystal and powder specimens.^{8,9} Of particular relevance to the present study is that the superconducting Er (Refs. 10 and 11) and Ho (Refs. 12 and 13) compounds as well as the nonsuperconducting Tb (Ref. 14) and Gd (Ref. 15) compounds all order in an incommensurate magnetic structure characterized by a propagation vector $\xi_m = (\xi_m, 0, 0)$, with $\xi_m \approx 0.55$ for all of these compounds. This observation is particularly important, since band theoretical calculations¹⁶ of the generalized electronic susceptibility of $\text{LuNi}_2\text{B}_2\text{C}$ show that there is strong Fermi-surface nesting in this compound with a nesting vector close to ξ_m . These results indicate that there is a common Fermi-surface nesting in these compounds, characterized by a nesting vector ξ_m , which is responsible for the

ordering of the rare-earth moments via the Ruderman-Kittel-Kasuya-Yosida (RKKY) mechanism. The existence of such a nesting suggests that strong Kohn anomalies should be observed in the dispersion curves of these compounds for wave vectors close to ξ_m . In addition, electronic band-structure calculations¹⁷⁻²⁰ suggest that these materials are conventional superconductors with relatively high electronic density of states at the Fermi level, E_F , and that there is a complex set of bands crossing E_F that are strongly coupled to the phonons and may be responsible for the superconducting properties of these compounds. Therefore, it appears that this family of compounds is ideal for the study of the subtle competition between lattice instabilities, superconductivity, and magnetic ordering.

Dervenas *et al.*²¹ measured the low-lying phonon dispersion curves of the Lu compound ($T_c \approx 16.5 \text{ K}$) along the $[\xi 00]$ and $[00\xi]$ symmetry directions and they found that the frequencies of the lowest-lying modes near ξ_m decrease with decreasing temperature and, as a result, the corresponding branches exhibit strong dips in the vicinity of this point at low temperatures. A similar study in the isomorphous Y compound was performed by Kawano *et al.*²² The softening of these modes is so significant that it was observed in phonon density of states measurements by Gompf *et al.*²³ as well as in the point-contact spectra of these compounds by Yanson *et al.*²⁴ In addition Kawano *et al.*²² performed a detailed study of the low-lying excitations in the Y compound as a function of temperature and magnetic field. They observed a dramatic change in the spectrum associated with the onset of superconductivity that includes a sharp feature at approximately 4 meV that they attributed to a "new" excitation.

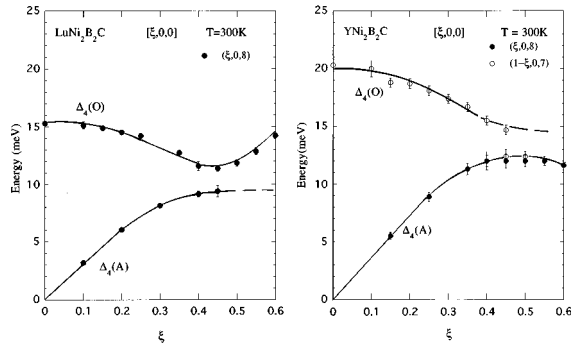


FIG. 1. Phonon dispersion of the two low-lying Δ_4 acoustic (A) and optic (O) branches measured, at 300 K, along the $[\xi 00]$ direction for $\text{LuNi}_2\text{B}_2\text{C}$ (left) and $\text{YNi}_2\text{B}_2\text{C}$ (right). The lines are used as a guide to the eye.

This interesting observation led us to perform a systematic study of these excitations as a function of temperature on the Lu and Y compounds. We already presented a brief account²⁵ of the results obtained in the experiments on the Lu compound. In this paper we present a more detailed account of these experiments as well as a comparison of the Lu and Y compounds.

II. EXPERIMENTAL DETAILS

The single crystals of $\text{LuNi}_2\text{B}_2\text{C}$ and $\text{YNi}_2\text{B}_2\text{C}$ used in the present experiment were grown at the Ames laboratory by the high-temperature flux technique as described elsewhere.²⁶ The as-grown crystals are platelets with the c axis perpendicular to their flat surface. Since the size of the crystals is relatively small (approximately $5 \times 5 \times 0.5 \text{ mm}^3$) for inelastic neutron scattering, most of the measurements on $\text{LuNi}_2\text{B}_2\text{C}$ were performed on a composite crystal, consisting of two crystals (mounted on a single holder) oriented to within 0.8° . Since the effect of the misorientation of the two $\text{LuNi}_2\text{B}_2\text{C}$ crystals is most pronounced for ξ between 0.375 and 0.425, where the abrupt decrease in the phonon frequencies occurs (see Fig. 1, Ref. 21), measurements in this region were performed with only one of the two $\text{LuNi}_2\text{B}_2\text{C}$ crystals. All measurements on $\text{YNi}_2\text{B}_2\text{C}$ were performed on a single crystal of this compound.

The measurements between 300 and 3.5 K were performed with the crystal placed in an He gas-filled aluminum can in a low-temperature refrigerator capable of regulating the temperature in this region to within 0.1 K. The measurements on the $\text{YNi}_2\text{B}_2\text{C}$ compound were extended up to 485 K and for these measurements the crystal was mounted in a high-temperature furnace. For all measurements on these compounds the crystal was mounted with the $[010]$ crystallographic direction perpendicular to the scattering plane.

The neutron-scattering experiments were performed using the variable incident neutron energy triple-axis spectrometers H-7 and H-8 at Brookhaven National Laboratory's high flux beam reactor and the constant incident neutron energy (14.7 meV) HB1A triple-axis spectrometer at the Oak Ridge National Laboratory's high flux isotope reactor. Pyrolytic graphite (PG), reflecting from the (002) planes, was used as monochromator and analyzer and a PG filter was used to eliminate higher-order contamination. On the H-7 and H-8 spectrom-

eters most of the data were collected using a fixed final neutron energy of 14.7 meV. The HB1A constant incident energy spectrometer was mainly used to study the temperature dependence (between 150 and 485 K) of the low-lying modes, in the vicinity of ξ_m , of the $\text{YNi}_2\text{B}_2\text{C}$ compound. Most of the data were collected with a collimation of 40-40-40-80 minutes of arc in the standard positions on the spectrometers.

III. EXPERIMENTAL RESULTS AND DISCUSSION

The phonon modes with frequencies below approximately 40 meV were studied systematically on the $\text{LuNi}_2\text{B}_2\text{C}$ compound at room temperature.^{21,27} Less extensive measurements were also made on the Y compound. The measured phonon frequencies were assigned to the various branches by comparing the measured intensities with calculations based on Born-von Kármán force-constant models. In the present investigation we studied in detail the temperature dependence of the $[\xi 00]$ acoustic and lowest-lying optic branches of $\text{LuNi}_2\text{B}_2\text{C}$ and $\text{YNi}_2\text{B}_2\text{C}$ in the vicinity of the nesting vector ξ_m , which is close to the zone-boundary point $G_1[\pi/a(1+a^2/c^2)]$ along this direction. By symmetry, the $[\xi 00]$ acoustic branch belongs to Δ_4 representation. Based on the analysis of the data using Born-von Kármán models, the lowest-lying optical branch along this direction was also assigned to the Δ_4 representation. No other branches of the same symmetry are close to these two branches. These calculations show that for small wave vectors these branches are purely transverse with atomic displacements parallel to the c axis; the displacements for all atoms in the acoustic modes are, of course, in phase, whereas in the optic modes the motion of the Lu atoms is out of phase with that of the other atoms. For larger wave vectors the displacements of the Lu and C atoms remain transverse but the Ni and B atoms develop a longitudinal component.

The temperature dependence of the two lowest-lying Δ_4 modes were studied by measurements in the Brillouin zones centered at (0,0,8) and (1,0,7). Figure 1 shows the dispersion of the Δ_4 optic (O) and acoustic (A) modes in the Lu and Y compounds at room temperature. The mass of Lu being nearly twice as large as that of Y, the energies of the modes are lower in $\text{LuNi}_2\text{B}_2\text{C}$ than in $\text{YNi}_2\text{B}_2\text{C}$. For $\xi < \xi_m$, both modes of the Lu compound are observed by measurements in the (008) Brillouin zone, whereas in the Y compound the optical mode is more easily observed by measurements in the (107) Brillouin zone. For $\xi > \xi_m$ the intensity of the acoustic and optical mode in the Lu and Y compounds, respectively, are very weak, and this is indicated by dotted lines in Fig. 1. In the vicinity of $\xi = \xi_m$, measurements in the (008) zone on the Y compound show, in addition to the acoustic mode, a peak at approximately 14 meV that was also observed by Kawano *et al.*²² and could be assigned to the optical branch (see discussion below).

Figure 2 shows the spectra of the interacting optic and acoustic mode in the vicinity of ξ_m at temperatures much higher than T_c . In the Y compound it is necessary to perform measurements at temperatures higher than room temperature in order to see clearly the mode interaction. At these high temperatures the optic mode (higher frequency mode) in both compounds is more intense than the acoustic mode.

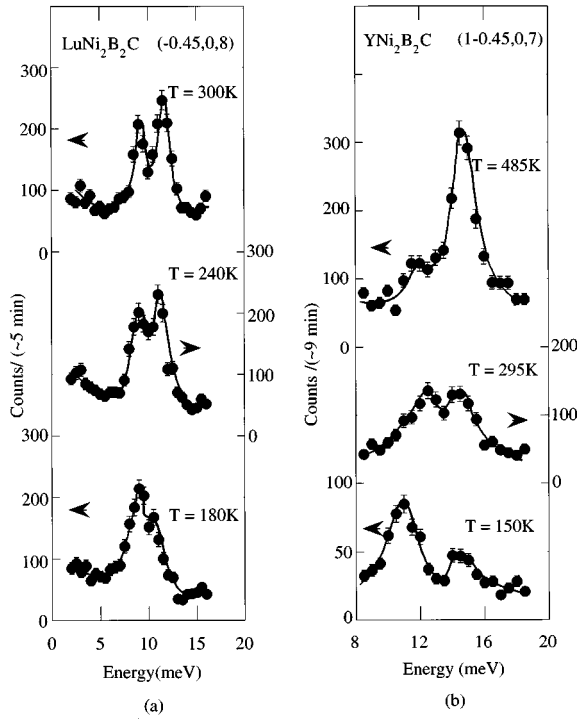


FIG. 2. Temperature dependence of the phonon spectra in the vicinity of ξ_m in (a) the Lu and (b) Y compounds. The right (left) panels were taken with energy gain (loss). The lines are used as a guide to the eye.

As T decreases the energy of the modes decrease and there is a transfer of intensity from the optic to the acoustic mode. For $T < 150$ K the two modes cannot be resolved and a broad feature is observed in the Lu compound. In the Y compound, a small peak at approximately 14 meV can be seen at temperatures below 150 K [see lowest panel of Fig. 2(b)]. As we mentioned earlier, this small peak was observed also by measurements in the (008) zone in the present experiments as well as those by Kawano *et al.*²² The intensity of this peak at 150 K is, however, approximately 60% lower than that expected from the intensity at 295 K [see Fig. 2(b)]. We believe that this peak is either the remnant of the optical mode or belongs to the Δ_1 representation, a possibility indicated by Born-von Kármán calculations.

The observed mode behavior *above* T_c both compounds is quite similar to that observed in materials with soft optic modes interacting with acoustic modes of the same symmetry. In the latter case their anticrossing behavior was formulated as a problem of mode coupling via anharmonic forces.^{27,28} The scattered neutron intensity in the coupled-mode problem is given by formula (A1) of the Appendix, and the effect of mode coupling for two different coupling constants is shown in Fig. 7. The first three top panels of Fig. 3 compare the spectra calculated using this simple model (see Appendix) with the observed spectra of $\text{LuNi}_2\text{B}_2\text{C}$ at temperatures well above T_c . In these calculations (see formula (A1) of the Appendix) the inelastic structure factors ($F_{1,2}$) of the two modes and the coupling constant (λ) are kept constant and only the linewidths (Γ_1, Γ_2) and frequencies (Ω_1, Ω_2) are adjusted to fit the experimental data. The left panels compare the measured and calculated spectra at (0.45, 0, 8) and the right panels those at (0.45, 0, 8.4) obtained

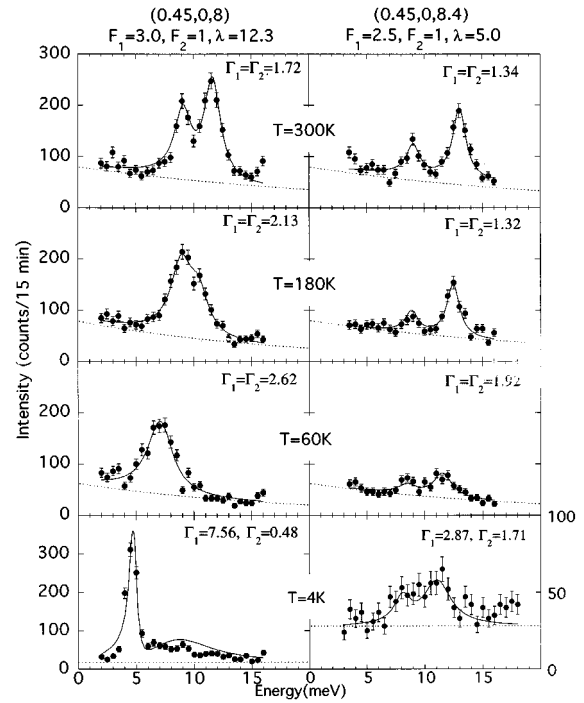


FIG. 3. Measured and calculated phonon profiles for several temperatures for (a) $\mathbf{Q} = (0.45, 0, 8)$ and (b) $\mathbf{Q} = (0.45, 0, 8.4)$. The calculations are based on the coupled-mode model described in the appendix.

for $\zeta = 0.4$ along a direction ($[00\zeta]$) that is perpendicular to $[\xi 00]$. For $T > T_c$ the model provides an adequate fit to the data in both cases. In particular it reproduces the merging of the two peaks at $T = 60$ K for the (0.45, 0, 8) mode as well as the two distinct peaks observed at (0.45, 0, 8.4) at all temperatures above T_c . It is probably of some interest to notice that the drastic change in the spectra occurring at temperature below T_c (see below) can be simulated in this simple model by a change in the width ($\Gamma_{1,2}$) of the two interacting modes, (this change being the largest for $\zeta = 0$) as shown in the lowest panels of Fig. 3. We would like to emphasize that the calculated curves in the lowest panels of Fig. 3 are not fits to the data, since below T_c no meaningful fits can be obtained (because of the large number of parameters involved); they were obtained by making appropriate choices for the widths, ($\Gamma_{1,2}$), so that these curves resemble the experimental profiles. It should also be pointed out that even above T_c the actual situation is much more complicated than the coupled-mode model, since the observed phonon anomalies in the Lu and Y compounds are due to the strong electron-phonon interaction via the nesting of the Fermi surface. As a result, the softening of these modes in the present case is mainly due to the sharpening of the Fermi-surface nesting feature as the temperature decreases. In addition, anharmonic effects may play some role as the compounds approach (but never achieve) a phase transformation at low temperatures.

As the temperature decreases below T_c , a spectacular change in the spectra is observed as was first reported by Kawano *et al.*²² for $\text{YNi}_2\text{B}_2\text{C}$ and Stassis *et al.*²⁵ for $\text{LuNi}_2\text{B}_2\text{C}$. Figure 4 shows our measurements on both compounds measured in the vicinity of T_c and well below T_c . In the vicinity of T_c , the Δ_4 optical and acoustic modes cannot

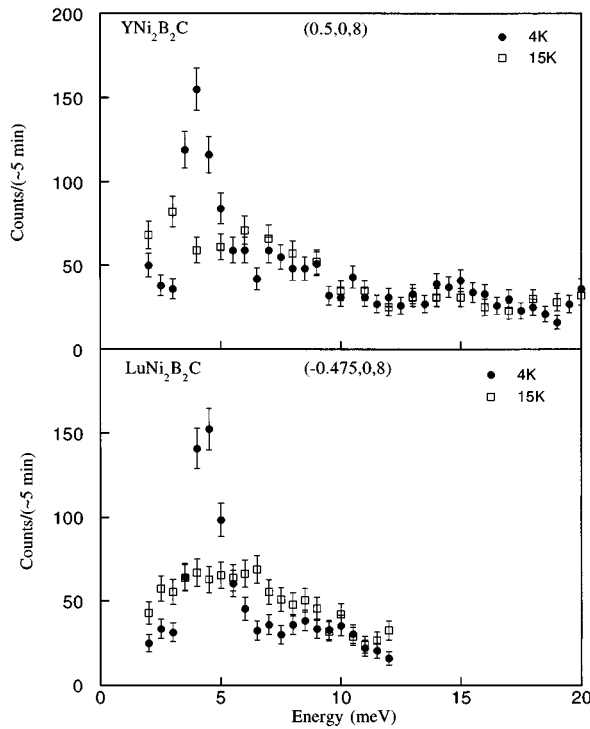


FIG. 4. Comparison of phonon profiles in $\text{YNi}_2\text{B}_2\text{C}$ (top) and $\text{LuNi}_2\text{B}_2\text{C}$ (bottom) obtained very near T_c (15 K) and below T_c (4 K).

be resolved and only a relatively broad feature is observed (see Fig. 4). Well below T_c the spectra are remarkably different. They consist of a sharp peak at approximately 4.5 meV with a weak shoulder at the higher energy side. Figure 5 illustrates the behavior of this sharp peak in $\text{LuNi}_2\text{B}_2\text{C}$ as a function of temperature [Fig. 5(a)] and ξ measured along $[\xi 00]$ [Fig. 5(b)]. The width and position of this sharp peak remain practically unchanged below T_c , its intensity decreases with increasing temperature, and it is practically indistinguishable from the background at a temperature close to T_c [Fig. 5(a)]. Although the full width at half maximum (FWHM) of this peak remains practically unchanged for ξ between 0.4 and 0.55, its intensity is maximum in the vicinity of $\xi = 0.475$ [Fig. 5(b)]. The energy of this sharp lower mode is minimum at approximately this wave vector ($\xi = 0.475$), and varies continuously with ξ between 0.4 and 0.6 between the energies observed at $\xi = 0.4$ and $\xi = 0.6$ for the Δ_4 acoustic branch. Figure 6 compares the dispersion along the $[00\xi]$ direction of the sharp peak and weak shoulder observed at low temperatures (right panel) with that of the Δ_4 modes at room temperature (left panel). The energies of the modes observed at 4 K (right panel) vary continuously with ξ , and as ξ increases the shoulder at the high-energy side becomes more well defined and, as a result, the two modes are clearly visible (Fig. 3). In particular, the study of the ξ dependence of the phonon modes clearly demonstrates that the single unresolved peak obtained, after the merging of the optical and acoustic modes, consists indeed of two phonon modes down to temperatures close to T_c (see third panel from top of Fig. 3). From this continuity of the modes we conclude that the sharp peak must be associated with the acoustic mode and the barely visible shoulder with the opti-

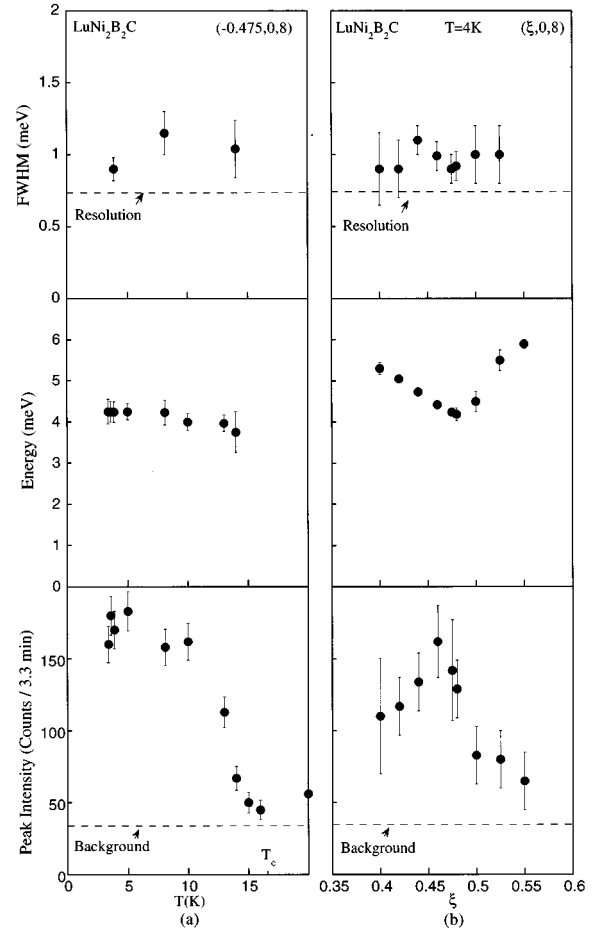


FIG. 5. (a) Temperature dependence of the FWHM, energy, and peak intensity of the sharp lower peak obtained at $(-0.475, 0, 8)$; (b) ξ dependence of the FWHM, energy, and peak intensity of the lower peak observed at 4 K.

cal mode. Notice (Fig. 6) that between 300 and 4 K the energies of both modes decrease by almost a factor of 2. The interpretation presented here is different from that proposed by Kawano *et al.*²² who associated the sharp peak observed at low temperatures with a “new” phononlike excitation that appears below T_c .

The experimental results clearly show that the origin of the dramatic change in the phonon spectra is the onset of superconductivity in these compounds. One of the direct effects of the superconducting gap opening is well understood and has been observed^{29,30} many years ago in superconducting Nb and Nb_3Sn . A phonon mode with energy lower than the superconducting gap 2Δ cannot decay by breaking Cooper pairs and therefore its lifetime is increased (linewidth narrowing) compared to its lifetime above T_c . In addition, because of the singularity at $\omega \cong 2\Delta$ in the polarizability of superconducting electrons, there is a shift in the phonon frequencies as well as a change in the phonon spectra as the temperature is decreased below T_c .^{31–33} Both the energy shifts and the phonon shapes depend on the position of the normal phonon frequency ω_n with respect to the superconducting gap 2Δ . It is interesting to note that for normal phonon frequencies close to $2\Delta(T)$ phonon shapes similar to the ones observed in the present experiment have been

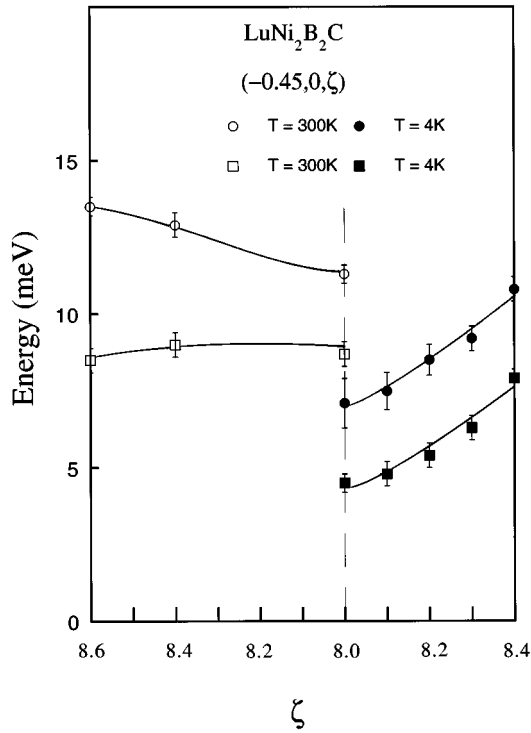


FIG. 6. Dispersion of the acoustic and optic Δ_4 modes measured along $[00\zeta]$ from $\mathbf{Q} = (-0.45, 0, 8)$ at $T = 300$ K and $T = 4$ K. The lines are used as a guide to the eye.

predicted.^{31,32} Actually, recent calculations by Allen *et al.*³³ yield phonon spectra almost identical to the low-temperature spectra shown in Fig. 4.

The above theoretical approaches^{31–33} are independent of the phonon wave vector whereas in the present experiments the anomalous phonon behavior is observed for phonon wave vectors close to the nesting vector ξ_m . Recently, however, Kee and Varma³⁴ found that the electronic polarizability for an extremum vector of the Fermi surface exhibits a pole for frequencies close to 2Δ . For a phonon with normal state frequency above 2Δ this leads to a delta function at ω slightly below 2Δ and a peak centered around the normal-state phonon frequency. Their spectra (see Fig. 2 of Ref. 34) when convoluted with the instrumental resolution are similar to those observed below T_c in the present experiments. The frequency of the observed sharp peak, on the other hand, does not follow the BCS temperature dependence of the superconducting gap as the Kee-Varma theory³⁴ predicts. Also it should be pointed out that the theory assumes that the opening of the superconducting gap does not affect appreciably the Fermi-surface nesting in these compounds as one would have expected.³⁵

In summary, in both compounds we observe a case of phonon softening of two branches, one acoustic and one optic, which belong to the same representation and therefore cannot cross by symmetry. Above T_c the observed anticrossing behavior of these branches is similar to a coupled-mode problem, and such a model gives a satisfactory explanation of the observed phonon profiles. Below T_c , the dramatic change in the observed spectra can be qualitatively understood in terms of the well-known linewidth narrowing and frequency shift associated with the opening of the supercon-

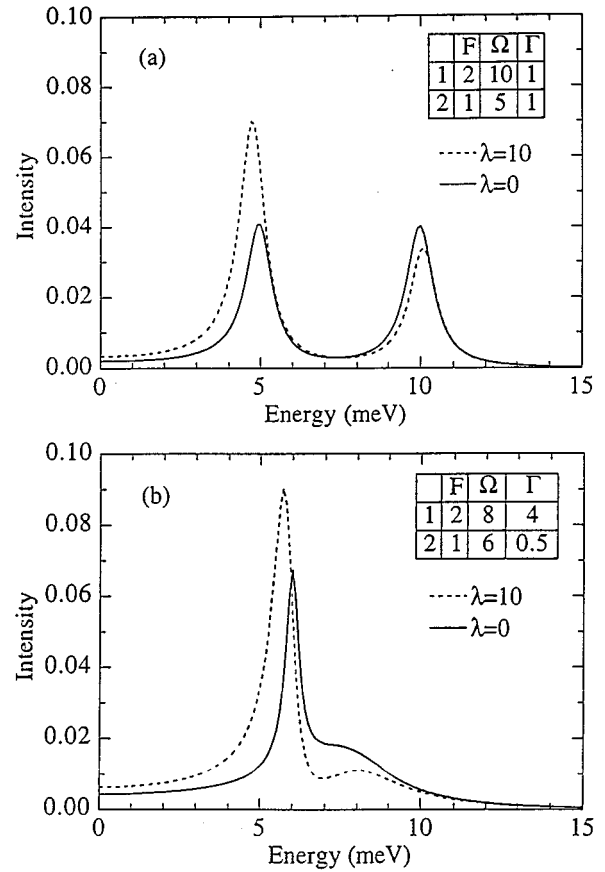


FIG. 7. (a) Calculated spectra for two modes with $\Gamma \ll \Omega$ in the uncoupled case ($\lambda = 0$) and with coupling $\lambda = 10$ showing transfer of intensity from one mode to another with increased coupling; (b) Calculated spectra for two modes with considerable spectral overlap.

ducting gap.^{31–34} More experimental and theoretical work is necessary, however, to relate the observed temperature dependence of the lowest-lying mode to the superconducting properties of these compounds.

ACKNOWLEDGMENTS

The authors are grateful to Dr. C. Varma, Dr. P. Allen, and Dr. S. K. Sinha for many stimulating discussions. Ames Laboratory is operated by the U.S. Department of Energy by Iowa State University under Contract No. W-7405-Eng-82. The work at Brookhaven National Laboratory was supported by the Department of Energy, Division of Materials Sciences, under Contract No. DE-AC02-76CH00016. Some of the experiments were performed at Oak Ridge National Laboratory, which is supported by the Department of Energy, Division of Materials Sciences, under Contract No. DE-AC05-96OR22464.

APPENDIX

The temperature-dependent behavior of the phonon modes of two branches that cannot cross by symmetry can be modeled as a mode-coupling problem by attributing the observed temperature dependence to anharmonic forces. The most convenient, for our purpose, formulation of the prob-

lem of two phonon modes interacting via anharmonic forces is that given by Harada and co-workers,²⁸ which was used to explain the asymmetric phonon profiles observed in ferroelectric BaTiO₃. The intensity distribution for two interacting modes, with frequencies Ω_1, Ω_2 and widths Γ_1, Γ_2 , is given, for neutron energy loss, by

$$I \sim [n(\omega) + 1] \frac{\omega}{(A^2 \omega^2 B^2)} \{[(\Omega_2^2 - \omega^2)B - \Gamma_2 A]F_1^2 + 2\lambda B F_1 F_2 + [(\Omega_1^2 - \omega^2)B - \Gamma_1 A]F_2^2\}, \quad (\text{A1})$$

where

$$A = (\Omega_1^2 - \omega^2)(\Omega_2^2 - \omega^2) - \omega^2 \Gamma_1 \Gamma_2,$$

$$B = \Gamma_1(\Omega_2^2 - \omega^2) + \Gamma_2(\Omega_1^2 - \omega^2).$$

In formula (A1),

$$n(\omega) = [\exp(\omega/kT) - 1]^{-1},$$

$F_{1,2}$ are the structure factors of modes 1 and 2, and λ is the coupling strength between the two modes.

Figure 7(a) shows the calculated spectra, at 300 K, of two coupled modes for the case $\lambda = 0$ (no coupling) and $\lambda = 10$. The two modes were taken to be well separated in energy and with linewidths much smaller than their energies. The inelastic structure factors were appropriately chosen in order to make the intensities of the two modes almost equal in the absence of coupling ($\lambda = 0$). As the coupling is turned on ($\lambda = 10$), there is considerable transfer of intensity from the upper to the lower mode. Since such transfer of intensity between modes is observed for $T > T_c$ in both the Y and Lu compounds (Fig. 2), it is clear that this simple coupled-mode model can be used to simulate the behavior of the Δ_4 modes above T_c . Figure 3 shows that this is indeed the case.

Figure 7(b) shows that, by choosing the energies and widths so that there is considerable overlapping of the two modes, one can obtain spectra qualitatively similar to those observed in both the Y and Lu compounds at temperatures below T_c (Fig. 4). The onset of superconductivity can therefore be simulated in this model by a change in the widths of the two interacting modes. Notice, however, that this change in the widths may be quite large (see Fig. 3).

*Present address: Brookhaven National Laboratory, Physics Dept., Bldg. 510B, P.O. Box 5000, Upton, NY 11973-5000.

¹R. Nagarajan, C. Maxamundar, Z. Hossain, S. K. Dhar, K. V. Golparrishnan, L. C. Gupta, C. Godart, B. D. Padalia, and R. Vijazarahgavan, Phys. Rev. Lett. **72**, 274 (1994).

²R. J. Cava, H. Takagi, H. W. Zandbergen, J. J. Krajewski, W. F. Peck, Jr., T. Siegrist, B. Batlogg, R. B. van Dover, R. J. Felder, K. Mizuhashi, J. O. Lee, H. Eisaki, and S. Uchida, Nature (London) **367**, 252 (1994).

³T. Siegrist, H. W. Zandbergen, R. J. Cava, J. J. Krajewski, and W. F. Peck, Jr., Nature (London) **367**, 254 (1994).

⁴R. Cava, H. Takagi, B. Batlogg, H. W. Zandbergen, J. J. Krajewski, W. F. Peck, Jr., R. B. van Dover, R. J. Felder, T. Siegrist, K. Mizuhashi, J. O. Lee, H. Eisaki, S. A. Cater, and S. Uchida, Nature (London) **367**, 146 (1994).

⁵H. Eisaki, H. Takagi, R. J. Cava, K. Mizuhashi, J. O. Lee, B. Batlogg, J. J. Krajewski, W. F. Peck, Jr., and S. Uchida, Phys. Rev. B **50**, 647 (1994).

⁶B. K. Cho, P. C. Canfield, and D. C. Johnston, Phys. Rev. B **52**, 3844 (1997).

⁷P. Dervenagas, J. Zarestky, C. Stassis, A. I. Goldman, P. C. Canfield, B. K. Cho, Physica B **212**, 1 (1995).

⁸C. Stassis and A. Goldman, J. Alloys Compd. **250**, 603 (1997).

⁹J. Lynn, J. Alloys Compd. **250**, 552 (1997).

¹⁰J. Zarestky, C. Stassis, A. I. Goldman, P. C. Canfield, P. Dervenagas, B. K. Cho, and D. C. Johnston, Phys. Rev. B **51**, 678 (1995).

¹¹S. K. Sinha, J. W. Lynn, T. E. Grigereit, Z. Hossain, L. C. Gupta, R. Nagarajan, and C. Godart, Phys. Rev. B **51**, 681 (1995).

¹²A. I. Goldman, C. Stassis, P. C. Canfield, J. Zarestky, P. Dervenagas, B. K. Cho, D. C. Johnston, Phys. Rev. B **50**, 9668 (1994).

¹³T. Vogt, A. Goldman, B. Sternlieb, and C. Stassis, Phys. Rev. Lett. **75**, 2628 (1995).

¹⁴P. Dervenagas, J. Zarestky, C. Stassis, A. I. Goldman, P. C. Canfield, B. K. Cho, Phys. Rev. B **53**, 8506 (1996).

¹⁵C. Detlefs, A. I. Goldman, C. Stassis, P. Canfield, B. K. Cho, J. P. Hill, D. Gibbs, Phys. Rev. B **53**, 6355 (1996).

¹⁶J. Y. Rhee, X. Wang, and B. N. Harmon, Phys. Rev. B **51**, 15 585 (1995).

¹⁷W. E. Pickett and D. J. Singh, Phys. Rev. Lett. **72**, 3702 (1994).

¹⁸L. F. Mattheiss, Phys. Rev. B **49**, 13 279 (1994).

¹⁹R. Coehoorn, Physica C **228**, 5671 (1994).

²⁰L. F. Mattheiss, T. Siegrist, and R. J. Cava, Solid State Commun. **91**, 587 (1994).

²¹P. Dervenagas, J. Zarestky, C. Stassis, A. I. Goldman, P. C. Canfield, B. K. Cho, Phys. Rev. B **53**, 8506 (1996).

²²K. Kawano, H. Yoshizawa, H. Takeya, and K. Kadowaki, Phys. Rev. Lett. **77**, 4628 (1996).

²³F. Gompf, W. Reichardt, H. Schober, B. Renker, and M. Bchgeister, Phys. Rev. B **55**, 9058 (1997).

²⁴I. K. Yanson, V. V. Fisun, A. G. M. Jansen, P. Wyder, P. C. Canfield, B. K. Cho, C. V. Tomy, and D. McK. Paul, Phys. Rev. Lett. **28**, 935 (1997).

²⁵C. Stassis, M. Bullock, J. Zarestky, P. Canfield, A. Goldman, G. Shirane, S. M. Shaprio, Phys. Rev. B **55**, 8678 (1997).

²⁶M. Xu, P. C. Canfield, J. E. Ostenson, D. K. Finnemore, B. K. Cho, Z. R. Wang, and D. C. Johnston, Physica C **227**, 321 (1994).

²⁷J. D. Axe, J. Harada, G. Shirane, Phys. Rev. B **1**, 1227 (1970).

²⁸J. Harada, J. D. Axe, G. Shirane, Phys. Rev. B **4**, 155 (1971).

²⁹J. D. Axe and G. Shirane, Phys. Rev. Lett. **30**, 214 (1973); Phys. Rev. B **8**, 1965 (1973).

³⁰S. M. Shapiro, G. Shirane, J. D. Axe, Phys. Rev. B **12**, 4899 (1975).

³¹H. G. Schuster, Solid State Commun. **13**, 1559 (1973).

³²R. Zeyher and G. Zwicknagl, Z. Phys. B **78**, 175 (1990).

³³P. B. Allen, V. N. Kostur, N. Takesue, and G. Shirane, Phys. Rev. B **56**, 5552 (1997).

³⁴H.-Y. Kee and C. M. Varma, Phys. Rev. Lett. **79**, 4250 (1997).

³⁵See, for instance, T. V. Ramakrishnan and C. M. Varma, Phys. Rev. B **24**, 137 (1981).